

PROCEEDINGS OF SPIE

[SPIDigitalLibrary.org/conference-proceedings-of-spie](https://spiedigitallibrary.org/conference-proceedings-of-spie)

The X-ray Surveyor Mission: a concept study

Jessica A. Gaskin, Martin C. Weisskopf, Alexey Vikhlinin, Harvey D. Tananbaum, Simon R. Bandler, et al.

Jessica A. Gaskin, Martin C. Weisskopf, Alexey Vikhlinin, Harvey D. Tananbaum, Simon R. Bandler, Marshall W. Bautz, David N. Burrows, Abraham D. Falcone, Fiona A. Harrison, Ralf K. Heilmann, Sebastian Heinz, Randall C. Hopkins, Caroline A. Kilbourne, Chryssa Kouveliotou, Ralph P. Kraft, Andrey V. Kravtsov, Randall L. McEntaffer, Priyamvada Natarajan, Stephen L. O'Dell, Robert Petre, Zachary R. Prieskorn, Andrew F. Ptak, Brian D. Ramsey, Paul B. Reid, Andrew R. Schnell, Daniel A. Schwartz, Leisa K. Townsley, "The X-ray Surveyor Mission: a concept study," Proc. SPIE 9601, UV, X-Ray, and Gamma-Ray Space Instrumentation for Astronomy XIX, 96010J (24 August 2015); doi: 10.1117/12.2190837

SPIE.

Event: SPIE Optical Engineering + Applications, 2015, San Diego, California, United States

The *X-ray Surveyor* Mission: A Concept Study

Jessica A. Gaskin^{*a}, Martin C. Weisskopf^a, Alexey Vikhlinin^b, Harvey D. Tananbaum^b, Simon R. Bandler^c, Marshall W. Bautz^d, David N. Burrows^e, Abraham D. Falcone^e, Fiona A. Harrison^f, Ralf K. Heilmann^d, Sebastian Heinz^g, Randall C. Hopkins^a, Caroline A. Kilbourne^c, Chryssa Kouveliotou^h, Ralph P. Kraft^b, Andrey V. Kravtsovⁱ, Randall L. McEntaffer^j, Priyamvada Natarajan^k, Stephen L. O'Dell^a, Robert Petre^c, Zachary R. Prieskorn^e, Andrew F. Ptak^c, Brian D. Ramsey^a, Paul B. Reid^b, Andrew R. Schnell^a, Daniel A. Schwartz^b, Leisa K. Townsley^e

^aNASA MSFC, ZP12, 320 Sparkman Drive, Huntsville, AL 35805; ^bSmithsonian Astrophysical Observatory, 60 Garden Street, Cambridge, MA 02138; ^cNASA Goddard Space flight Center, 8800 Greenbelt Rd, Greenbelt, MD 20771; ^dMassachusetts Institute of Technology, 77 Massachusetts Ave, Cambridge, MA 02139; ^ePennsylvania State University, University Park, PA 16802; ^fCalifornia Institute of Technology, 1200 E California Blvd, Pasadena, CA 91125; ^gUniversity of Wisconsin, Madison, WI 53706; ^hGeorge Washington University, 2121 I St NW, Washington, DC 20052; ⁱUniversity of Chicago, 5801 S Ellis Ave, Chicago, IL 60637; ^jUniversity of Iowa, Iowa City, IA 52242; ^kYale University, New Haven, CT 06520

ABSTRACT

NASA's *Chandra* X-ray Observatory continues to provide an unparalleled means for exploring the high-energy universe. With its half-arcsecond angular resolution, *Chandra* studies have deepened our understanding of galaxy clusters, active galactic nuclei, galaxies, supernova remnants, neutron stars, black holes, and solar system objects. As we look beyond *Chandra*, it is clear that comparable or even better angular resolution with greatly increased photon throughput is essential to address ever more demanding science questions—such as the formation and growth of black hole seeds at very high redshifts; the emergence of the first galaxy groups; and details of feedback over a large range of scales from galaxies to galaxy clusters. Recently, we initiated a concept study for such a mission, dubbed *X-ray Surveyor*. The *X-ray Surveyor* strawman payload is comprised of a high-resolution mirror assembly and an instrument set, which may include an X-ray microcalorimeter, a high-definition imager, and a dispersive grating spectrometer and its readout. The mirror assembly will consist of highly nested, thin, grazing-incidence mirrors, for which a number of technical approaches are currently under development—including adjustable X-ray optics, differential deposition, and new polishing techniques applied to a variety of substrates. This study benefits from previous studies of large missions carried out over the past two decades and, in most areas, points to mission requirements no more stringent than those of *Chandra*.

Keywords: X-ray Astronomy, X-ray optics, X-ray gratings, X-ray detectors

1. INTRODUCTION

The *X-ray Surveyor* is one of the large astrophysics mission concepts that may be studied by NASA in preparation for the 2020 U.S. Decadal Survey¹. Consistent with the 2013 Astrophysics Roadmap², the goals for the observatory are: excellent (at least *Chandra*-like) angular resolution, while providing a factor of 30-100 higher throughput; significantly larger field of view than *Chandra* for sub-arcsec imaging; and a suite of next-generation science instruments, including a microcalorimeter, a High Definition Imager and high-efficiency gratings for spectroscopy in the soft X-ray band. With these capabilities, the *X-ray Surveyor* will be able to detect and characterize extremely faint objects and study physical processes in a very wide range of astrophysical settings.

The baseline *X-ray Surveyor* Mission concept is in response to the “Planning for the 2020 Decadal Survey: An Astrophysics Division white paper” that was presented to the community by the NASA Astrophysics Director in January of 2015. In this white paper, the Astrophysics community was asked to comment on a small list of candidate missions to

*jessica.gaskin@nasa.gov

the NASA Program Analysis Groups (PAGs). The report(s) generated by the PAGs will be submitted to the NASA Advisory Council (NAC) Astrophysics Subcommittee, who will report to the Astrophysics Division for selection of the mission concepts to study as input for the 2020 Decadal Survey. These more formal studies will be carried out by appointed Science and Technology Definition Teams (STDTs), and will be assigned to NASA Centers to manage.

2. COMPELLING SCIENCE

It is a great challenge to understand the complexities of the universe in which we live. NASA Astrophysics is driven by three defining questions: How did we get here? How does the universe work? Are we alone? A multi-wavelength approach is required to address these questions, and astronomers have demonstrated that X-ray observations provide an essential element to this quest. The *X-ray Surveyor* mission will provide unique insights into the evolution of the universe from early epochs to the present, while probing and elucidating underlying physical processes on scales from cosmological to atmospheres of nearby stars and planetary systems. To achieve great gains, particularly in sensitivity, over currently operating and proposed X-ray observatories, the *X-ray Surveyor* utilizes revolutionary X-ray optics and cutting-edge instrumentation.

3. BASELINE CONCEPT

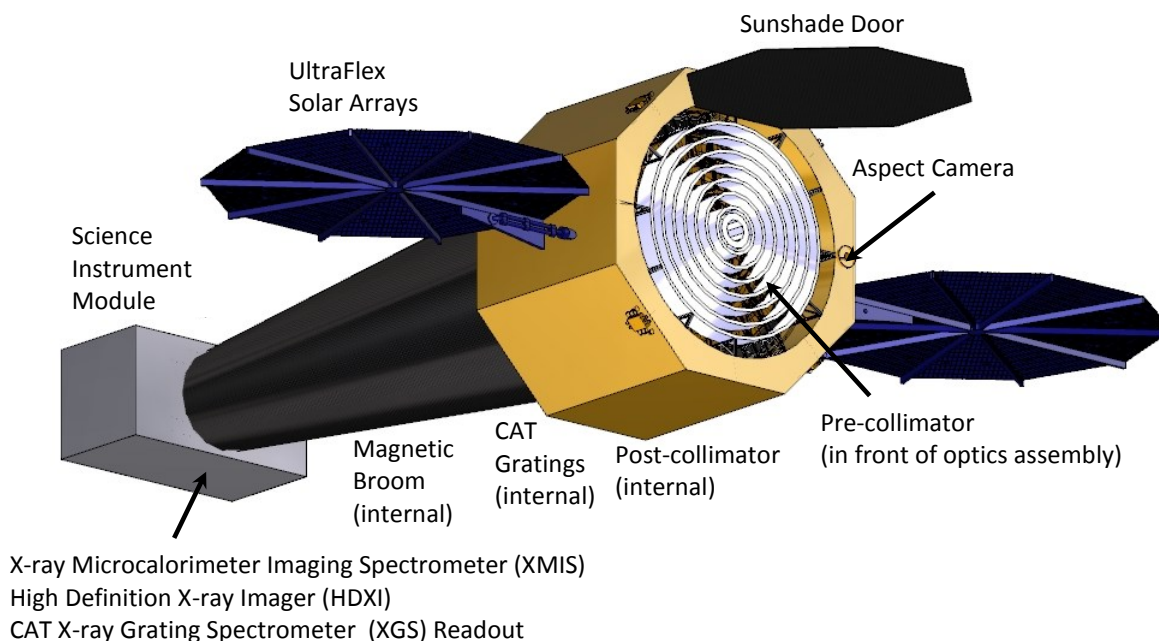


Figure 1. Artist's conception of the *X-ray Surveyor* baseline mission concept.

An initial concept study for the *X-ray Surveyor* mission was carried-out by the Advanced Concept Office (ACO) at Marshall Space Flight Center (MSFC), with a strawman payload and related requirements that were provided by an Informal Mission Concept Team (IMCT), comprised of MSFC and Smithsonian Astrophysics Observatory (SAO) scientists plus a diverse cross-section of the X-ray community. The study included a detailed assessment of the requirements, a preliminary design (Figure 1), a mission analysis, and a preliminary cost estimate and leveraged relevant concept definitions for other large area missions carried out over the past two decades, such as Con-X, AXSIO and IXO. In many areas, the *X-ray Surveyor* mission requirements are no more stringent than those of *Chandra*, and so heritage systems and design features were utilized when possible. The *X-ray Surveyor* focal length, for example, is approximately the same as *Chandra*'s, which limits the spacecraft requirements and results in a Chandra-like cost.

With its half-arcsecond angular resolution, *Chandra* has provided an unparalleled means for exploring the high-energy universe; deepening our understanding of astronomical systems as diverse as galaxy clusters, active galaxies, normal and starburst galaxies, supernova remnants, normal stars, planets, and solar system objects.^{3,4,5} As we look beyond *Chandra*, it is clear that comparable angular resolution combined with greatly increased photon throughput is essential for addressing the key questions outlined in the 2010 Decadal Survey and in the 2013 NASA Astrophysics Roadmap.

4. OPTICS PERFORMANCE AND CONFIGURATION

The substantial gains in the detection sensitivity limit of the *X-ray Surveyor* require X-ray mirrors that combine large throughput with high angular resolution to avoid X-ray source confusion and background contamination. High angular resolution is also critical for providing unique identifications of faint X-ray sources.

An initial optical design for the *X-ray Surveyor* mirror system incorporates a segmented system similar to *Con-X*^{6,7} and *AXSIO*⁸, but with a 3 m diameter, a 10 m focal length and a 0.5 arcsec Half Power Diameter (HPD) at 1 keV. A Wolter-Schwarzschild (W-S) prescription is used, which provides superior off-axis imaging to a Wolter-I^{9,10}. The result is a ~15 arcmin diameter field-of-view with 1 arcsec or better HPD. An approximation to the optimally curved focal plane will be incorporated into the imaging sensor (comprised of many active pixel sensor chips) to further improve off-axis performance¹⁰. When convolved with nominal as built mirror performance and the ‘curved’ focal plane, off-axis imaging (mirror + aberrations) at 1 keV is less than 1 arcsec (HPD) over a ~20 arcmin diameter field-of-view.

Large mirror effective area is accomplished by nesting 292-segmented shells into 42 individual mirror modules, which are then assembled into a larger structure with a 3 m outer diameter (Figure 2).

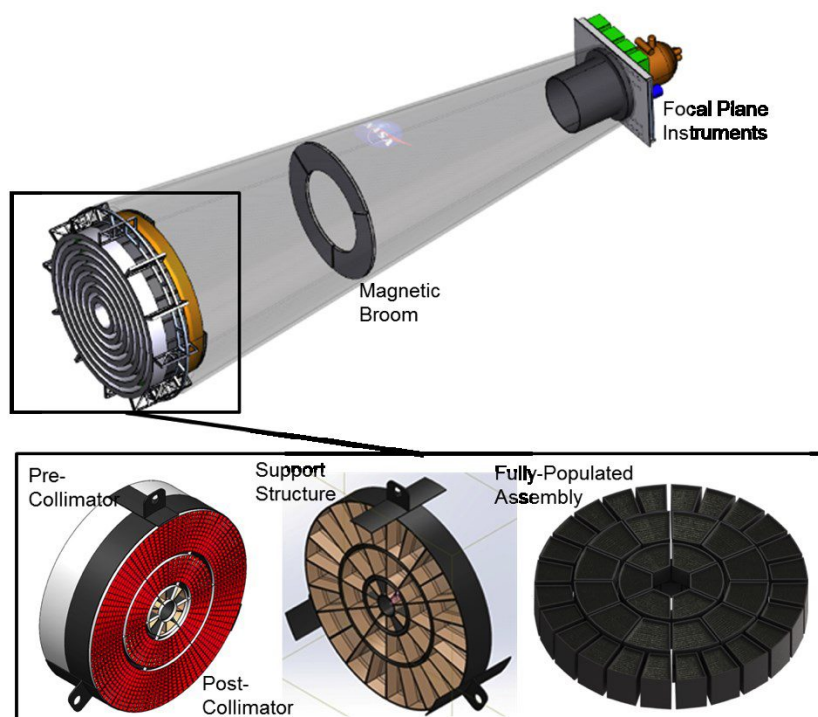


Figure 2. (Top) Nearly transparent view of *X-ray Surveyor* telescope. The mirror assembly, magnetic ring and focal plane are visible. (Lower-Left) Diagram of the Pre- and Post-thermal collimators. (Lower-Center) Diagram of the optics structure that supports 42 mirror modules. (Lower-Right) Diagram of a fully populated mirror assembly. The full assembly includes 292-segmented, nested mirror shells.

The calculated effective area includes structural obscuration, misalignments, particulate contamination, scatter and ray-traced vignetting as a function of energy and field position (Figure 3). The on-axis effective area is 2.3 m^2 at 1 keV.

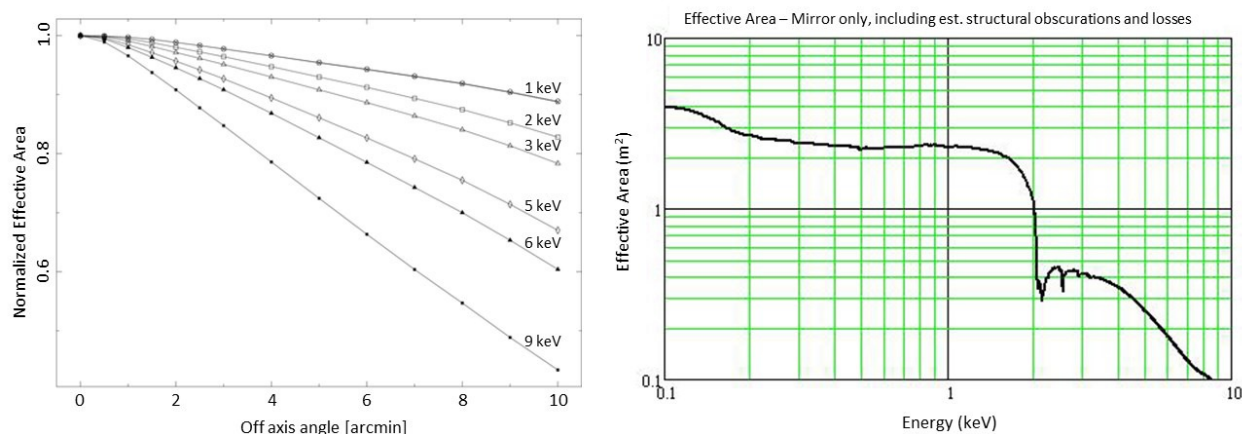


Figure 3. (Left) Vignetting as a function of energy and field. (Right) On-axis effective area prediction for *X-ray Surveyor*. The area at 1 keV is 2.3 m^2 . This calculated effective area includes structural obscuration, misalignments, particulate contamination and scatter. This is roughly 30x that of the Chandra High Resolution Mirror Assembly (HRMA).

Maintaining sub-arcsec resolution over a large effective area (few-square meters) is a challenging, but not impossible task. There are a number of on-going efforts focused on developing technologies for the fabrication of lightweight, high-resolution X-ray mirrors. These include both active (e.g. piezoelectric actuator deposition^{11,12} and magnetorestrictive optics) and passive (e.g., differential deposition^{13,14}, ion implantation^{15,16} and low stress single crystal silicon mirrors¹⁷) methods to achieve the desired imaging. The two technologies that this concept study focused on were the piezoelectric actuator deposition and differential deposition.

Adjustable Optics (Active)

One technique for fabricating adjustable optics is being developed at SAO/PSU, in which a continuous thin film (1.5 μm) of piezoelectric material is sputter deposited with independently addressable electrodes to the back (convex) side of a slumped glass substrate. Low ($< 10 \text{ V}$) DC voltage applied thru the piezoelectric film's thickness produces an in-plane stress in the piezoelectric, resulting in localized bending of the mirror. This technique enables efficient correction of the mirror figure for: fabrication errors, mounting induced distortions, and on-orbit changes due to the thermal environment.

Piezoelectric actuator deposition and operation has been demonstrated on both a 10 cm diameter flat test mirrors and on 10 cm x 10 cm cylindrical mirrors (22 cm radius of curvature)^{18,19}. Deterministic figure change with this technique has been successfully demonstrated on a 10 cm diameter flat mirror. A thin film of 75 piezo actuators (10 x 5 mm cells) was deposited on the surface of the flat and these actuators were operated together to apply a deterministic figure in the central 75 x 50 mm region. The input slope error (prior to correction) was 5.2 arcsec rms, and the residual slope error post-correction was measured to be 0.81 arcsec rms, or a factor of > 6 improvement²⁰.

Differential Deposition (Passive)

Differential deposition is a process by which a filler material is selectively deposited on a mirror's surface to improve low-to-mid spatial frequency figure errors that degrade the angular resolution of the optics. These errors are present due to the fabrication and alignment process. To determine where and how much of the filler material should be applied, a 'hit' map is created by measuring the uncorrected mirror profile and comparing it to the desired profile. One group at MSFC is working on this, and uses nickel vapor deposited via sputtering (or other) to deposit the filler material onto the optic while the optic is translated at a pre-determined set of velocities¹³. Another group at Reflective X-ray Optics

Corporation in New York is also working on this^{21,22}. Both groups are making progress applying differential deposition to thin substrates (including polished silicon).

Recent results at MSFC have shown that full-shell mirrors can be corrected to better than half that of their original HPD (as proven through profile metrology measurements) in a single pass. Corrections may require 2 or more deposition passes, depending on the initial quality of the mirror segment. This technique works best when applied to the mid-spatial frequency errors; however, it can be applied to low-frequency errors as well²³ and can be applied to mirror segments and full-shell replicated optics^{23,24}. Improved mirror fabrication techniques are also being employed to address the low-frequency errors.

5. FOCAL PLANE INSTRUMENTS

The high-resolution optics are complimented by high-resolution gratings and instruments located at a focal length of 10 m. The focal plane instruments include the X-ray Microcalorimeter Imaging Spectrometer (XMIS), the High Definition X-ray Imager (HDXI) and the X-ray Grating Spectrometer (XGS) readout. Critical Angle Transmission (CAT) gratings can be inserted and retracted into and out of the X-ray beam. XMIS and HDXI are mounted on a translation table that allows them to be swapped with each other at the telescope focus. The CAT-XGS readout is mounted in a fixed location at the focal plane. The *X-ray Surveyor* instruments are currently under development by several research groups and so can be classified as cutting edge; the key is that this X-ray instrumentation exploits the new telescope's properties. As with the optics, none of these instruments currently exist in a form that can meet all of the *X-ray Surveyor* requirements but there is significant activity and substantial progress towards their development.^{25,26,27,28,29,30}

X-ray Microcalorimeter Imaging Spectrometer (XMIS)

X-ray microcalorimeters are actively being developed for astrophysics missions; *Astro-H* (Soft X-ray Spectrometer)³¹ and *Athena* (XMS)³² are two examples. The *X-ray Surveyor* conceptual design will, likewise, employ an X-ray microcalorimeter, dubbed XMIS, at its focal plane. The XMIS instrument is capable of providing high-spectral resolution images, well matched to the proposed optics (Table 1). XMIS is designed to utilize transition-edge sensor (TES) or magnetically coupled calorimeters (MCC) in pixel array-sizes approaching 100 kilo-pixels.

Table 1. List of preliminary XMIS requirements for the *X-ray Surveyor* concept.

Parameter	Goal
Energy Range	0.2 – 10 keV
Field-of-View	5 arcmin x 5 arcmin (minimum)
Energy Resolution	< 5 eV
Pixel Size / array size (10-m focal length)	50 μ m pixels (1 arcsec) / 300 x 300 pixel array
Count Rate Capability	1 c/s per pixel

To reduce the number of sensors read out to a manageable scale, the most promising detector geometries are those in which a thermal sensor such a TES or MCC can read out a sub-array of 20-25 individual 1arcsec pixels.

An example approach that involves the use of TESs for thermal multiplexing is with Hydras, or single-channel position-sensitive TESs.^{33,34} Hydras consist of a single TES coupled to multiple absorber pixel elements (illustrated in Figure 4)³³. Each pixel has a different thermal coupling, which allows for identification via pulse shape discrimination. Multiple Hydras can be arrayed to read out the full detector. Recent results from a 3 x 3 absorber pixel array³⁵, where all 9 pixels were read out with a single TES gave 2.4 eV FWHM-resolution at 6 keV. Pixels were 65 μ m square and had a thickness of 5 μ m and TES pitch was 75 μ m³⁶, illustrating the potential for reading out larger, 10⁵ – sized pixel arrays.

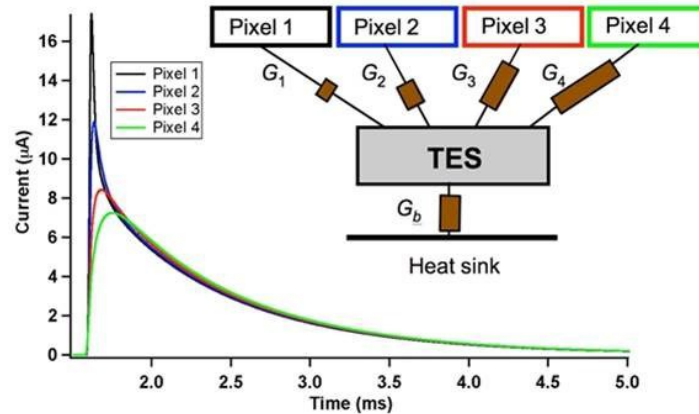


Figure 4. (Left) The TES can read out multiple absorbers or ‘pixels’ to decrease the number of readouts (Hydra). Using absorbers with different thermal conductance to that of the sensor allows one to distinguish the pulse shape from each pixel. (Right) Diagram of the 3 x 3 absorber array with a single TES mounted beneath the central absorber. G1-G4 are the internal link/thermal couplings between the TES and the pixels.

If the aforementioned approach is successful, then the number of sensors needed to be read out is the same as is currently proposed for the X-ray Integral Field Unit instrument on *Athena* (~3840). Therefore the multiplexing technologies currently being developed for *Athena* could be directly transferable to this spectrometer. Alternative read-out approaches also exist that utilize microwave Superconducting QUantum Interference Devices (SQUIDs) coupled to each sensor in resonator circuits in the GHz frequency range. A comprehensive summary of X-ray microcalorimeter developments for X-ray Astrophysics missions can be found in the literature³⁷.

High-Definition X-Ray Imager (HDXI)

The HDXI focal plane instrument for the *X-ray Surveyor* will provide a large field of view while simultaneously providing fine pixel resolution and high readout rate (instrument goals are listed in Table 2.) To satisfy these requirements, multiple active pixel sensor technologies are under consideration, including hybrid Complementary Metal Oxide Semiconductor or CMOS (PSU/Teledyne^{38,39}), monolithic CMOS (SAO/Sarnoff), and 3-D tiered/layered bonded Si (MIT/Lincoln Labs^{41,42,43}) (Figure 5). HDXI requirements are similar to those of the Wide Field Imaging Spectrometer designed for the SMART-X concept, and a full description of competing technologies has been reviewed in the literature⁴⁴.

All of the detector development efforts are making good progress towards meeting individual goals listed in Table 2, but no single CMOS development was chosen for the *X-ray Surveyor* baseline concept since it is not clear which of the technologies will most effectively meet all of the requirements. *X-ray Surveyor*’s mass, power, and cost estimates were determined with values for the HDXI that would enable any of the three detector technologies to fit within the estimates.

Table 2. List of preliminary HDXI requirements for the *X-ray Surveyor* concept.

Parameter	Goal
Energy Range	0.2 – 10 keV
Field of View	22 arcmin x 22 arcmin
Energy Resolution	37 eV @ 0.3 keV, 120 eV @ 6 keV (FWHM)
Quantum Efficiency	> 90% (0.3-6 keV), > 10% (0.2-9 keV)
Pixel Size / Array Size	<16 µm (< 0.33 arcsec/pixel) / 4096 x 4096 (or equivalent)
Frame Rate	> 100 frames/s (full frame), > 10000 frames/s (windowed region)
Read Noise	< 4e ⁻ rms

Silicon-based sensors, such as those based on CMOS technology, have several properties that make them ideal candidates for a mission such as the *X-ray Surveyor*; including potential for high quantum efficiency (QE) for soft x-rays, excellent angular resolution over a large field of view, excellent spectral resolution, high frame rates and high radiation tolerance. CMOS-based detectors also generally operate with relatively low power, compared to that of CCDs³⁸.

Hybrid CMOS detectors, such those being developed by PSU/Teledyne, have shown high quantum efficiency (QE) across the entire soft X-ray bandpass, including reasonably high QE in the upper end of this energy range where response to Fe K α becomes important³⁹.

Fine angular resolution imaging over a wide field of view is achieved by using a silicon sensor array with small pixels. Fabricating small pixels is not unreasonable; however, combined with a large depletion depth (which is related to achieving high QE) the charge sharing between pixels can become an issue. To achieve the goal of < 0.33 arcsec/pixel across the field of view of the 10 m focal length *X-ray Surveyor* telescope, < 16 μm pixels are required. This is a realizable goal, in that the group at PSU/Teledyne is currently developing a 12.5 μm pixel pitch hybrid CMOS device. This device design borrows from the existing Teledyne HyViSITM imager with flight heritage⁴⁵, while providing small pixels and improved amplifier technology that will be tested over the next 3 to 5 years. The SAO/Sarnoff monolithic CMOS sensor has achieved a pixel size of 16 μm ⁴⁰, and the MIT/Lincoln Labs effort has demonstrated a pixel size of 8 μm ⁴⁶, but each of these detectors still require development in order to achieve the other *X-ray Surveyor* requirements along with the small pixels. This work is progressing.

To support the *X-ray Surveyor*'s large field of view, one could use a single 4096 x 4096 pixel device with 16 μm pixels. However, in order to accommodate the curvature of the focal surface, a preferred design is to use multiple abutable detectors with a bowl-shaped tilt, as was done for the *Chandra* ACIS instrument⁴⁷. A possible configuration would be to tile 1024 x 1024 pixel devices using 21 detectors arranged in a 5x5 grid pattern with the 4 corners removed. A detector design with 15 μm pixels would then cover a 26 arcmin x 26 arcmin field of view when arranged in this way, thus exceeding the 22 arcmin x 22 arcmin goal.

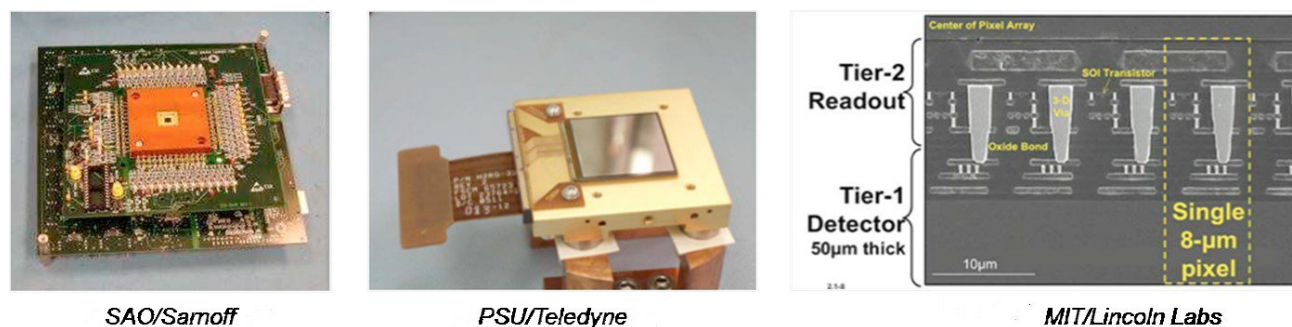


Figure 5. Images of active CMOS developments at SAO/Sarnoff (monolithic sensor), PSU/Teledyne (hybrid sensor) and MIT/Lincoln Labs (Active Pixel Sensor).

X-ray spectral resolution is impacted by several factors, including read noise, inter-pixel capacitance crosstalk, and charge spreading within the photodetector. Improvements in pixel design have already shown that we can lower read noise and reduce capacitive coupling to negligible levels, and planned developments show promise that these improvements will be possible within small pixels and with even faster readouts.

To satisfy the *X-ray Surveyor* readout requirements and mitigate pile-up, the HDXI must be capable of much faster frame rates than current CCD X-ray imagers. High frame rates in CMOS-based detectors are achieved using highly parallel readout circuitry architectures, and by reading out windows of the detector at faster rates than the full detector. These windows can be chosen to overlap with the bright sources in a field of view, while the full frame gets read out in parallel. Current X-ray CMOS detectors are already capable of reading out small windows of the detector at speeds that meet the *X-ray Surveyor* window mode requirements, but more developments are needed to enable this simultaneously with lower noise and faster full-frame readouts. Future event-driven detector designs and/or increased parallel output designs with small-pixel detectors will enable the realization of all of these requirements simultaneously.

X-ray photon counting active pixel sensors, such as CMOS devices, also have a higher radiation tolerance than their more traditional CCD counterparts. CCDs are particularly sensitive to radiation damage, as evidenced by the Advanced CCD Imaging Spectrometer on *Chandra* (ACIS)⁴⁸, the result of which is degradation of detector performance (e.g., increased charge transfer inefficiency) over time. However, CMOS sensors are much more radiation tolerant since the charge is transferred directly from the detector pixel into the readout circuitry associated with that pixel, as opposed to transferring the charge across the detector as is done with CCDs. The main mechanism for degradation of energy resolution due to radiation is displacement damage in the silicon lattice caused by proton irradiation. This produces charge traps that capture electrons in the charge packet produced by absorption of an X-ray. The effect is roughly proportional to the distance through which the charge must be transferred in the silicon before the packet size is measured. In a CCD this is of order 10 mm, while in an active pixel sensor this is of order 0.1 mm; hence the active pixels sensors are ~100x less sensitive to proton damage than are CCDs.

X-ray Grating Spectrometer (XGS)

Critical-Angle Transmission (CAT) and Off-Plane Reflection Gratings (OPG) are two candidate technologies for the *X-ray Surveyor*. The combination of high-efficiency gratings blazed to high orders and square-meter collecting-area optics will provide unprecedented performance in the x-ray band below ~ 2 keV; complementing the XMIS performance in the harder x-ray band. Initial conceptual designs for the *X-ray Surveyor* assume grating spectroscopy effective area on the order of 4,000 cm², and spectral resolving power $R = \lambda/\Delta\lambda$ of up to 5,000, is achieved by covering less than 50% of the optics aperture with retractable grating arrays.

As a starting point, the CAT grating technology, currently being developed at MIT³⁰ was incorporated into the *X-ray Surveyor* baseline concept. These gratings are freestanding and supported by a coarse grating array structure designed to fold into and out of the optical path, and by a hexagonal mesh with a ~1 mm pitch (L2), and also by a finer bar- support mesh with a ~5 μ m period (L1), shown in Figure 6. The gratings are made from silicon-on-insulator wafers using a combination of advanced lithography, pattern transfer, and dry and wet etching techniques. Recently fabricated samples have shown record-high absolute diffraction efficiencies > 30% in high orders. Increasing grating depth will lead to even higher efficiencies.

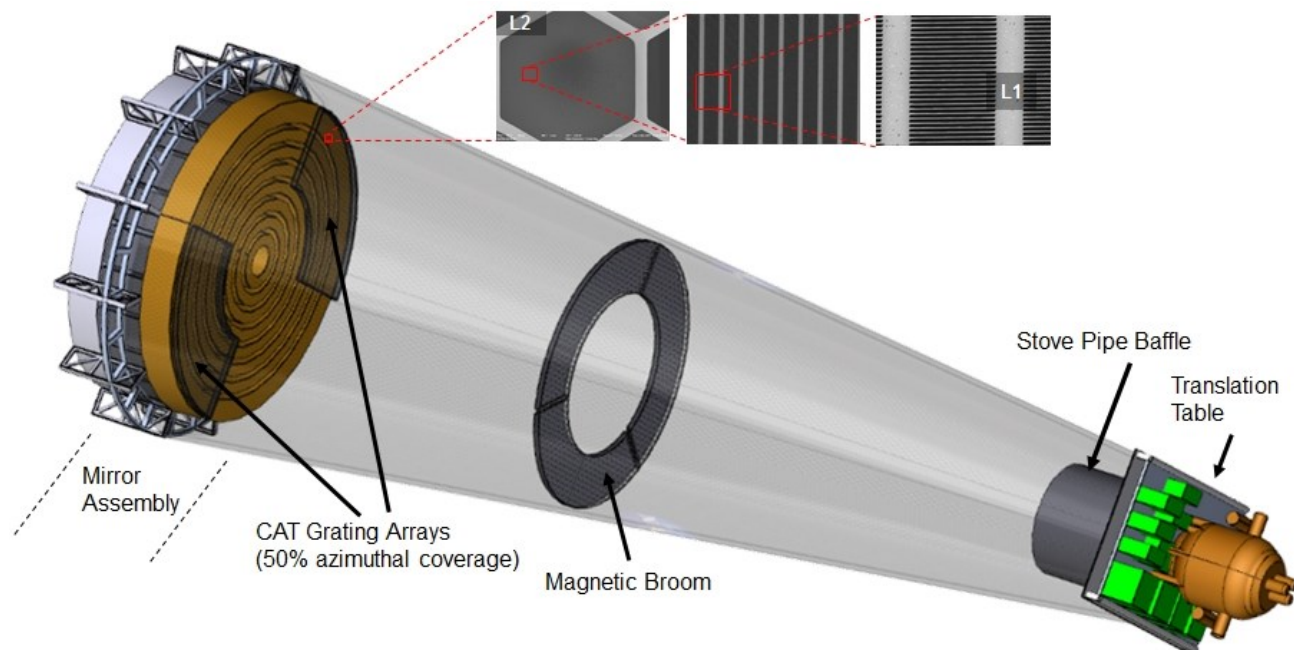


Figure 6. Transparent image of the *X-ray Surveyor* optical bench showing the placement of the CAT gratings with respect to the telescope optics. The readout cameras are not shown, but would be mounted in fixed positions on either side of the translation table. The 3 micrographs at the top of the image show the L2 hexagonal support mesh and the finer L1 bar-structure that supports the freestanding gratings. The magnetic broom, which is designed to sweep electrons reflecting through the optics assembly out of the optical path, is also shown.

Compared to *Chandra*'s HETG or *XMM-Newton*'s RGS instruments, CAT gratings promise higher diffraction efficiency (Figure 7), and use sub-aperturing in combination with blazing (utilizing higher diffraction orders) to provide increased spectral resolving power.

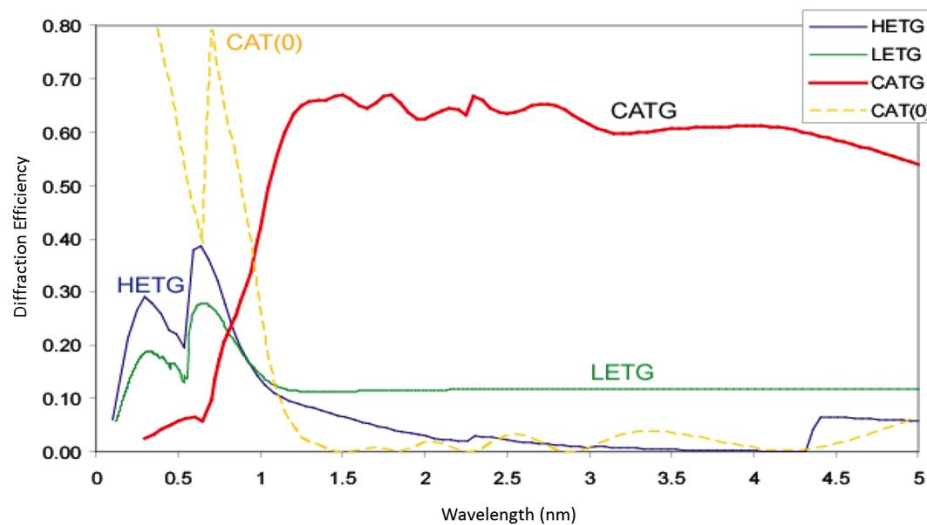


Figure 7. Comparison between the theoretical maximum for a particular CAT grating (CATG) design diffraction efficiency (losses from support structures neglected) on *X-ray Surveyor* and HETG (High Energy Transmission Gratings) and LETG (Low Energy Transmission Gratings) currently operating on *Chandra*. The CAT gratings are 6 μm -deep (no blockage), and CAT(0) is 0th order transmission.

Two linear readout cameras (CCD or CMOS-based) in the focal plane, offset from an imaging detector at the imaging focus, will detect the grating spectra and separate spatially overlapping diffraction orders of different wavelengths.

Recent progress has been made in the fabrication of the CAT gratings, with a clear path forward for improving the diffraction efficiencies (e.g. using a smaller blaze angle and improved etching process) and yield. Similarly, significant progress has been made with the OPGs. A novel fabrication approach allows for high density, radially grooved, blazed gratings for high throughput and high resolving power⁴⁹. OPGs have shown very high diffraction efficiency while tests on prototypes of the new fabrication method have shown promise of efficiencies > 50% at given energies^{49,50}. These gratings have also been tested for spectral resolving power and have achieved resolutions >3000 during testing with NASA Goddard Space Flight Center X-ray optics in the MSFC Stray Light Facility⁵¹. In addition, the alignment tolerances for OPGs have been quantified^{52,53}. Using these tolerances as a baseline, OPGs have been aligned into a module and tested with Silicon Pore Optics modules to demonstrate an aligned spectrometer^{54,55}. Blazed, radial gratings, matching flight-like properties, were also tested to demonstrate the capability for high spectral resolving power⁵⁶.

6. SPACECRAFT

The spacecraft includes structure and mechanisms, propulsion, thermal systems, avionics, guidance and navigation control, electrical and power systems, and a science instrument translation table. *X-ray Surveyor* spacecraft management of mechanisms, thermal control, power switching, communication interfaces, and storage of scientific data have all been defined in this concept, and many are based on or derived from those of the *Chandra* Observatory, which reduces risk and helps to constrain spacecraft costs.

7. MISSION PROFILE

The *X-ray Surveyor* has been baselined for a Sun-Earth L2 Halo Orbit. The nominal mission duration is 5 years, with 20 years of on-board consumables. Based on experience with missions such as *Chandra* and *XMM-Newton* in high earth orbits, it is reasonable to expect a mission extending for 20 years or longer without having to design for that level in terms of components and subsystems. The estimated volume and mass with 30% margins, which is based on a Master Equipment List (MEL), meet the requirements of launch on an Atlas V 551 (or similar class vehicle). End-of-Life drift-away disposal will round out the mission.

8. COST ESTIMATE

The analogy-based NASA/Air Force Cost Model (NAFCOM) was employed to cost the spacecraft subsystems in this estimate, using the *Chandra* spacecraft as the analogy. The cost for the X-ray telescope assembly is a bottoms-up input from the Informal Mission Concept Team and costs for the scientific instruments were derived using JPL's NASA Instrument Cost Model (NICM). All costs are presented in 2015 dollars based on NASA's "New Start Inflation Indices for 2015". Fee, program support and vehicle integration were included in the cost. A 35% reserve was applied to the spacecraft and the X-ray Telescope Assembly. The instrument estimates from NICM were compiled at the 70% confidence level, which is deemed to be an appropriate and sufficient level of confidence consistent with NASA Procedural Requirement 7120.5E. Facilities cost to support pre-flight calibration are still under investigation and have not been included. For the purposes of this study, all costs are based on all of the necessary technologies having a Technology Readiness Level 6 at the time the mission enters the development phase and no later than the preliminary design review. A summary of the cost break-down is given in Table 3.

Table 3. Preliminary cost estimates for the baseline *X-ray Surveyor* mission concept. These will be further refined with future studies, but gives a rough estimate indicating *Chandra*-like costs.

Spacecraft	\$1,650M
X-ray Telescope Assembly and Instruments	\$866M
Pre-Launch Operations, Planning and Support	\$196M
Launch with Atlas V 551	\$240M
Total	\$2,952M

9. DISCUSSION

The next large NASA mission to be prioritized in the 2020 Astrophysics Decadal Survey must be scientifically compelling and technologically capable; surpassing the accomplishments of past and current missions. The *X-ray Surveyor* will accomplish this by utilizing heritage successes from *Chandra* combined with emerging technologies that promise dramatically improved capability. Specifically, the *X-ray Surveyor* will maintain *Chandra*'s sub-arcsecond angular resolution while dramatically improving sensitivity (the effective area is ~50x that of *Chandra* HRMA + ACIS, over 0.5 – 2 keV). Sub-arcsec imaging will be maintained over a large field-of-view (22 arcmin x 22 arcmin) and high-resolution spectroscopy with a spectral resolving power of R=5000 (0.2 – 1.2 keV) and R=1200 (6 keV) will also be possible.

Enabled by its sensitivity, angular resolution, and spectroscopic capabilities, the frontier science that *X-ray Surveyor* will address includes fundamental studies of the roles which central black holes play in the evolution of galaxies, plasma physics, gas dynamics and relativistic flows in a variety of astronomical objects, and the nature of the first accretion light

in the Universe. A broad (and very incomplete) range of additional topics where *X-ray Surveyor* will provide unique information includes: detailed studies of AGN feedback in clusters, groups, and galaxies with the ability to distinguish between sound wave and turbulent heating mechanisms; tracing winds and jets while deciphering the overall gas flow picture around supermassive black holes; unraveling the processes by which AGN jets are powered, collimated, and re-accelerated; unfolding the interactions of supernova blasts, shocks, and ejecta with circumstellar and interstellar material as well as mapping particle acceleration in supernova remnants and pulsar wind nebulae; and probing coronal activity in stars of all ages along with extending our understanding of star-planet interactions.

The *X-ray Surveyor* concept study summarized here is a first step towards proving feasibility of such a mission. All crucial technologies for the telescope and focal plane instrumentation are actively being developed. Progress of many of these developments is reported at this conference. Designing the focal length to be approximately that of *Chandra* and by utilizing *Chandra* heritage systems for the spacecraft, results in a *Chandra*-like cost.

10. ACKNOWLEDGEMENTS

We wish to acknowledge detailed contributions from Dr. Stephen Smith (NASA GSFC) and Dr. Kiranmayee Kilaru (NASA MSFC). We would also like to recognize the Advanced Concept team (led by Randall Hopkins and Andrew Schnell) and Cost team (led by Spencer Hill) at NASA MSFC for their work on developing the *X-ray Surveyor* mission concept.

¹ http://science.nasa.gov/media/medialibrary/2015/01/02/White_Paper_-_Planning_for_the_2020_Decadal_Survey.pdf

² <http://science.nasa.gov/science-committee/subcommittees/nac-astrophysics-subcommittee/astrophysics-roadmap/>

³ Santos-Lleo, M., Schartel, N., Tananbaum, H., Tucker, W., Weisskopf, M. C. "The first decade of science with *Chandra* and XMM-Newton," *Nature*, 462 (7276), 997-1004 (2009).

⁴ Weisskopf, M. C., "The *Chandra* X-Ray Observatory: progress report and highlights," *Proc. SPIE*, 8443, 84430Y (2012).

⁵ Tananbaum, H., Weisskopf, M. C., Tucker, W., Wilkes, B., Edmonds, P., "Highlights and discoveries from the *Chandra* X-ray Observatory" *Reports on Progress in Physics*, 77 (6), article id. 066902 (2014)

⁶ Petre, R., Zhang, W., David A., Saha, T., Stewart, J., Hair, J. H., Nguyen, D., Podgorski, W. A., Davis, Jr., W. R., Freeman, M. D., Cohen, L. M., Schattenburg, M. L., Heilmann, R. K., Sun, Y., Forest, C. R., "Constellation-X spectroscopy X-ray telescope (SXT)," *Proc. SPIE* 4851, X-Ray and Gamma-Ray Telescopes and Instruments for Astronomy, 433 (March 10, 2003).

⁷ O'Dell, S. L., Jones, W. D., Ramsey, B. D., Engelhaupt, D. E., Smith, D. S., Cohen, L. M., Van Speybroeck, L. P., "Development of Constellation-X optics technologies at MSFC," *Proc. SPIE* 4012, X-Ray Optics, Instruments, and Missions III, 316 (July 18, 2000).

⁸ Bookbinder, J. A., Smith, R. K., Bandler, S., Garcia, M., Hornschemeier, A., Petre, R., Ptak, A., "The Advanced X-ray Spectroscopic Imaging Observatory (AXSIO)." *Proc. SPIE*, pp. 844317-844317 (2012).

⁹ Chase, R. C. and Van Speybroeck, L. P., "Wolter-Schwarzschild Telescopes for X-ray Astronomy," *Applied Optics*, 12 (5), 1042-1044 (1973)

¹⁰ Allured, R., et al., In Prep.

¹¹ Reid, P. B., Murray, S. S., Trolier-McKinstry, S., Freeman, M., Juda, M., Podgorski, W., Ramsey, B., and Schwartz, D., "Development of adjustable grazing incidence optics for Generation-X," In *SPIE Astronomical Telescopes+ Instrumentation*, 70110V-70110V, International Society for Optics and Photonics, (2008)

¹² Reid, P. B., Davis, W., O'Dell, S., Schwartz, D. A., Trolier-McKinstry, S., Wilke, R. H. T. and Zhang, W., "Generation-X mirror technology development plan and the development of adjustable x-ray optics," In *SPIE Optical Engineering+ Applications*, 74371F-74371F, International Society for Optics and Photonics, (2009)

¹³ Kilaru, K., An Investigation of differential deposition for figure corrections in grazing incidence x-ray optics: A Dissertation, University of Alabama in Huntsville (2010).

¹⁴ Kilaru, K., Ramsey, B. D., Gubarev, m., Gregory, D., "Differential deposition technique for figure corrections in grazing-incidence x-ray optics," *Opt. Eng.*, 50 (10), 106501 (September 28, 2011)

¹⁵ Chalifoux, B., Heilmann, R. K., Schattenburg, M. L., "Shaping of thin glass X-ray telescope mirrors using air bearing slumping and ion implantation," *Proc. SPIE*, 9144, 91444D (2014).

- ¹⁶ Chalifoux, B., Wright, G., Heilmann, R. K., Schattenburg, M. L., "Ion implantation for figure correction of thin x-ray telescope mirror substrates," This proceedings. Paper 9603-51 (2015)
- ¹⁷ Riveros, R. E., Bly, V. T., Kolos, L. D., McKeon, K. P., Mazzarella, J. R., Miller, T. M., Zhang, W. W., "Fabrication of single crystal silicon mirror substrates for x-ray astronomical missions," Proc. SPIE 9144, Space Telescopes and Instrumentation 2014: Ultraviolet to Gamma Ray, 914445 (July 25, 2014).
- ¹⁸ Cotroneo, V., Davis, W. N., Marquez, V., Reid, P. B., Schwartz, D. A., Johnson-Wilke, R. L., Troler-McKinstry, S. E., Wilke, R. H. T., "Adjustable grazing incidence x-ray optics based on thin PZT films," Proc. SPIE 8503, Adaptive X-Ray Optics II, 850309 (October 19, 2012).
- ¹⁹ Reid, P. B., Aldcroft, T. L., Cotroneo, V., Davis, W., Johnson-Wilke, R. L., McMudroch, S., Ramsey, B. D., Schwartz, D. A., Troler-McKinstry, S., Vikhlinin, A., Wilke, R. H. T., "Development status of adjustable grazing incidence optics for 0.5 arc second x-ray imaging," Proc. SPIE 8861, Optics for EUV, X-Ray, and Gamma-Ray Astronomy VI, 88611Q (September 26, 2013).
- ²⁰ Allured, R., Ben-Ami, S., Cotroneo, V., Marquez, V., McMudroch, S., Reid, P., Troler-McKinstry, S., Vikhlinin, A., Wallace, M., "Improved control and characterization of adjustable x-ray optics," This Proceedings, paper 9603-53 (2015).
- ²¹ Windt, D. L., Conley, R., "Two-dimensional differential deposition for figure correction of thin-shell mirror substrates for x-ray astronomy," This proceedings, paper 9603-47 (2015)
- ²² Weisskopf, M. C., Gaskin, J. A., Tananbaum, H., Vikhlinin, A., "Beyond Chandra: the x-ray Surveyor," Proc. SPIE 9510, EUV and X-ray Optics: Synergy between Laboratory and Space IV, 951002 (May 12, 2015).
- ²³ Kilaru, K., Atkins, C., Ramsey, B.D., Gubarev, M., Broadway, D.M., "Progress in differential deposition for improving the figures of full-shell astronomical grazing incidence x-ray optics," This proceedings, paper 9603-46
- ²⁴ Atkins, C., Kilaru, K., Ramsey, B.D., Broadway, D.M., Gaskin, J.A., Gubarev, M.V., O'Dell, S.L., Zhang, W.W., "Differential deposition correction of segmented glass x-ray optics," This Proceedings, Paper 9603-46 (2015).
- ²⁵ Betancourt-Martinez, G. L., Adams, J., Bandler, S., Beiersdorfer, P., Brown, G., Chervenak, J., Doriese, R., Eckart, M., Irwin, K., Kelley, R., Kilbourne, C., Leutenegger, M., Porter, F. S., Reintsema, C., Smith, S., & Ullom, J., "The transition-edge EBIT microcalorimeter spectrometer," Proc. SPIE 9144, 3U 11 pp (2014)
- ²⁶ Griffith, C. V., Falcone, A. D., Prieskorn, Z. R., Burrows, D. N., "The speedster-EXD: a new event-triggered hybrid CMOS x-ray detector," Proc. SPIE, 9154, 0W 9 pp. (2014).
- ²⁷ Kenter, A., Kraft, R., Gauron, T., & Murray, S. S., "Monolithic CMOS imaging x-ray spectrometers", Proc. SPIE 9154, 91540J, 11pp (2014)
- ²⁸ Prigozhin, G., Foster, R., Suntharalingam, V., Kissel S., LaMarr, B. and Bautz, M., "Measurement results for and X-ray 3-D-integrated active pixel sensor," Proc. SPIE, 7742, 77421I (2010)
- ²⁹ Heilmann, R. K., Bruccoleri, A. R., Guan, D., & Schattenburg, M. L., "Fabrication of large-area and low mass critical-angle x-ray transmission gratings," Proc. SPIE 9144, 1A 8 pp (2014)
- ³⁰ Heilmann, R. K., Bruccoleri, A. R., Schattenburg, M. L., "High-efficiency blazed transmission gratings for high-resolution soft x-ray spectroscopy," These Proceedings, paper 9603-25 (2015).
- ³¹ Mitsuda, K., Kelley, R., Boyce, K., Brown, G., Costantini, E., DiPirro, M., Ezoe, Y., Fujimoto, R., Gendreau, K., den Herder, J. W., Hoshino, A., Ishisaki, Y., Kilbourne, C., Kitamoto, S., McCammon, D., Murakami, M., Murakami, H., Ogawa, M., Ohashi, T., Okamoto, A., Paltani, S., Pohl, M., Porter, F. S., Sato, Y., Shinozaki, K., Shirron, P., Sneiderman, G., Sugita, H., Szymkowiak, A., Takei, Y., Tamagawa, T., Tashiro, M., Terada, Y., Tsujimoto, M., de Vries, C., Yamaguchi, H., Yamasaki, N., "The high-resolution X-ray Microcalorimeter Spectrometer System for the XRS on Astro-H," Proc. SPIE, 7732, 77321I (July 29, 2010).
- ³² Barret, D., den Herder, J. W., Piro, L., Ravera, L., Den Hartog, R., Macculi, C., Barcons, X., Page, M., Paltani, S., Rauw, G., Wilms, J., Ceballos, M., Duband, L., Gottardi, L., Lotti, S., de Plaa, J., Pointecouteau, E., Schmid, C., Akamatsu, H., Bagliani, D., Bandler, S., Barbera, M., Bastia, P., Biasotti, M., Branco, M., Camón, A., Cara, C., Cobo, B., Colasanti, L., Costa-Krämer, J.L., Corcione, L., Doriese, W., Duval, J.M., Fàbrega, L., Gatti, F., de Gerone, M., Guttridge, P., Kelley, R., Kilbourne, C., van der Kuur, J., Mineo, T., Mitsuda, K., Natalucci, L., Ohashi, T., Peille, P., Perinati, E., Pigot, C., Pizzigoni, G., Pobes, C., Porter, F., Renotte, E., Sauvageot, J.L., Sciortino, S., Torrioli, G., Valenziano, L., Willingale, D., de Vries, C., van Weers, H., "The hot and energetic universe: The x-ray integral flux unit (X-IFU) for Athena+," arXiv:1308.6784 [astro-ph.IM] (30 Aug 2013).
- ³³ Smith, S. J., Bandler, S. R., Brekosky, R. P., Brown, A. -D., Chervenak, J. A., Eckart, M. E., Finkbeiner, F. M., Kelley, R. M., Kilbourne, C. A., Porter, F. S., Figueroa-Feliciano, E., "Development of arrays of position sensitive

microcalorimeters for Constellation-X,” Proc. SPIE, Space Telescopes and Instrumentation 2008: Ultraviolet to Gamma Ray, vol. 7011, article 701126, 2008.

³⁴ Smith, S. J., Bandler, S. R., Brekosky, R. P., Brown, A. -D., Chervenak, J. A., Eckart, M. E., Figueroa-Feliciano, E., Finkbeiner, F. M., Iyomoto, N., Kelley, R. L., Kilbourne, C. A., Porter, F. S., Sadleir, J. E., “Development of position-sensitive transition-edge sensor X-ray detectors,” IEEE Transactions on Applied Superconductivity, 19(3) 451-455 (2009).

³⁵ Smith, S. J., “Implementation of complex signal processing algorithms for position-sensitive microcalorimeters,” Nucl. Instr. and Meth. A, 602(2), 537-544 (2009)

³⁶ Smith, S. J., Adams, J. S., Bandler, S. R., Busch, S. E., Chervenak, J. A., Eckart, M. E., Ewin, A. J., Finkbeiner, F. M., Kelley, R. L., Kilbourne, C. A., Lee, S. J., Porst, J. -P., Porter, F. S., Sadleir, J. E., Wassel, E. J., “Multi-absorber transition-edge sensors for x-ray astronomy,” Unpublished results presented at the 15th International Workshop on Low Temperature Detectors (LTD-15), California Institute of Technology, Pasadena, CA, 2013.

³⁷ Kilbourne, C., Bandler, S., Chervenak, J., Doriese, W. B., Hilton, G., Irwin, K., Kelley, R., Porter, F. S., Reintsema, C., Ulom, J., “Enabling Technologies for the High-Resolution Imaging Spectrometer of the Next NASA X-Ray Astronomy Mission - Options, Status, and Roadmap,” A response to RFI NNH11ZDA018L: Concepts for the Next X-ray Astronomy Mission submission 28 (2011).

³⁸ Prieskorn, Z., Griffith, C. V., Bongiorno, S. D., Falcone, A. D., Burrows, D. N., “Characterization of Si hybrid CMOS detectors for use in the soft x-ray band,” NIM A, 717, 83-89 (2013)

³⁹ Prieskorn, Z. R., Bongiorno, S. D., Burrows, D. N., Falcone, A. D., Griffith, C. V., Nikoleyczik, J., “Soft x-ray quantum efficiency of silicon hybrid CMOS detectors,” Proc. SPIE, 9154, 915410 (2014)

⁴⁰ Kenter, A., Kraft, R., Gauron, T., Murray, S. S., “Monolithic CMOS Imaging X-ray Spectrometers,” Proc. SPIE, 9154, 91540J (Jul 2014)

⁴¹ Suntharalingam, V., Rathman, D., Progozhin, G., Kissel, S., Bautz, M., “Back-illuminated three-dimensionally integrated CMOS image sensors for scientific applications,” Proc. SPIE 6690, 669009-1 (2007).

⁴² Prigozhin, G., Foster, R., Suntharalingam, V., LaMarr, B. and Bautz, M., “Measurement results from an x-ray 3D-integrated active pixel sensor,” Proc. SPIE, 7742, 77421I (2010)

⁴³ LaMarr, B., Bautz, M., Foster, R., Kissel, S., Prigozhin, G. and Suntharalingam, V., “Interpixel crosstalk in a 3D-integrated active pixel sensor for x-ray detection,” Proc. SPIE, 7742, 77422B (2010)

⁴⁴ Murray, S., Bautz, M., Burrows, D., Falcone, A., Kenter, A., Kraft, R., & Park, P. A. “Active Pixel X-ray Sensor Technology Development for SMART-X Focal Plane.”

http://beyondstein.nasa.gov/studies/rfi/Murray_Active_Pixel_Sensors.pdf

⁴⁵ Bai, Y., Bajaj, J., Beletic, J., Farris, M., Joshi, A., Lauxtermann, S., Petersen, A., Williams, G., “Teledyne Imaging Sensors: Silicon CMOS imaging technologies for x-ray, UV, visible and near infrared,” SPIE Astronomical Telescopes+ Instrumentation. International Society for Optics and Photonics (2008).

⁴⁶ Suntharalingam, V., Rathman, D., Progozhin, G., Kissel, S., Bautz, M., “Back-illuminated three-dimensionally integrated CMOS image sensors for scientific applications,” Proc. SPIE, 6690, 669009-1 (2007).

⁴⁷ Nousek, J. A., Garmire, G. P., Ricker, G. R., Bautz, M. W., Levine, A. M., Collins, S. A., “Matching a curved focal plane with CCDs: Wide field imaging of glancing incidence x-ray telescopes,” Proc. SPIE, 0818, Current Developments in Optical Engineering II, 296 (January 1, 1987).

⁴⁸ O’Dell, S. L., Blackwell, W., Cameron, R., Minow, J., Morris, D., Spitzbart, B., Swartz, D., Virani, S., Wolk, S., “Managing radiation degradation of CCDs on the Chandra X-ray Observatory,” Proc. SPIE, 4851 (2003).

⁴⁹ McEntaffer, R. L., DeRoo, C., Scultz, T., Gantner, B., Tutt, J., Holland, A., O’Dell, S., Gaskin, J., Kolodziejczak, J., Zhang, W., Chan, K.-W., Biskach, M., McClelland, R., Iazikov, D., Wang, X., Koecher, L., “First results from a next-generation off-plane X-ray diffraction grating,” Exp. Astron., 36, 389, 7 pp (2013)

⁵⁰ Miles, D. M., Marlowe, H. R., McCoy, J. A., Peterson, T. J., McEntaffer, R. L., Schultz, T. B., Tutt, J. H., Rogers, T. D., Laubis, C., Scholze, F., “Diffraction efficiency measurements of radially-profiled off-plane gratings,” Proc. SPIE, These proceedings, paper 9603-37 (2015).

⁵¹ McEntaffer, R. L., et al., In prep (2015).

⁵² Allured, R., & McEntaffer, R. L., “Analytical alignment tolerances for off-plane reflection grating spectroscopy,” Exp. Astron., 36, 661, 17 pp (2013)

⁵³ Allured, R., Donovan, B. D., & McEntaffer, R. L., “Alignment tolerances for off-plane reflection grating spectrometry: Theoretical calculations and laboratory techniques,” Proc. SPIE, 8861, 88611C, 12 pp (2014)

⁵⁴ Marlowe, H., et al., "Performance Testing of a Novel Off-plane Reflection Grating and Silicon Pore Optic Spectrograph at PANTER," JATIS, accepted (2015)

⁵⁵ Allured, R., Donovan, B. D., Burwitz, V., Cheimets, P. N., DeRoo, C. T., Hartner, G., Marlowe, H. R., Hertz, E., Menz, B., Smith, R. K., Tutt, J. H., "X-ray and optical alignment approaches to off-plane reflection gratings," Proc. SPIE, These proceedings, paper 9603-36 (2015)

⁵⁶ DeRoo, C.T., et al., "Line Spread Functions of Blazed Off-Plane Gratings Operated in the Littrow Mounting," JATIS, submitted (2015)